Chemical Engineering Journal 307 (2017) 353–363

Contents lists available at ScienceDirect

Chemical Engineering Journal

journal homepage: www.elsevier.com/locate/cej

Comparison of sorption and desorption studies of heavy metal ions from biochar and commercial active carbon

D. Kołodyńska [a,*], J. Krukowska [a], P. Thomas [b]

[a] Department of Inorganic Chemistry, Faculty of Chemistry, Maria Curie-Skłodowska University, M. Curie Skłodowska Sq. 2, 20-031 Lublin, Poland
[b] Coaltec Energy USA, Inc., United States

HIGHLIGHTS

- Sorption/desorption studies of Cu(II), Zn(II), Cd(II) and Zn(II) on AC and BC were carried out.
- 180 min, pH 5, temperature 293 K, dose 0.1 g proved to be optimal values for sorption process.
- BC was characterized by better adsorption capacities than commercial AC.

GRAPHICAL ABSTRACT

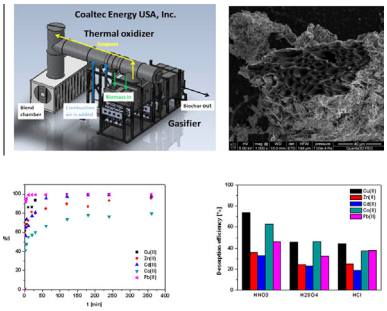

ARTICLE INFO

Article history:
Received 28 June 2016
Received in revised form 18 August 2016
Accepted 19 August 2016
Available online 20 August 2016

This article is dedicated to Professor Zbigniew Hubicki on the occasion of his 70th birthday.

Keywords:
Biochar
Active carbon
Pyrolysis
Sorption
Desorption

ABSTRACT

In the first stage on the effectiveness of various operating factors such as: adsorbent dose, contact time, solution pH, initial concentration and temperature on the sorption of heavy metal ions of Cu(II), Zn(II), Cd (II), Co(II) and Pb(II) were carried out using the commercial active carbon Purolite AC 20 and biochar. It was found that the sorption capacity increases with the increasing phase contact time and concentration of the initial solution. It was found that biochar removes more efficiently heavy metal ions from aqueous solutions than the activated carbon. Sorption kinetic data provide a complex mechanism of sorption and better fit of the pseudo second order model than the pseudo first order and the intraparticle diffusion ones. In the second stage the desorption of the above mentioned heavy metal ions from the biochar and commercial activated carbon was conducted. It was proved that biochar has excellent properties and can be used as a sorbent of multi-use 0.1 M HNO_3 was the best eluent for desorption of heavy metal ions in the sorption/desorption studies in the third stage. In order to characterize the mechanism of sorption/desorption for both biochar and activated carbon, the Brunauer Emmett Teller surface area was determined and point of zero charge was measured. Moreover, the elemental analysis and the Fourier transform infrared spectroscopy were applied. The thermogravimetric and derivative thermogravimetric analyses were conducted.

1. Introduction

Heavy metals produced by different branches of industry are hazardous for health and life of humans and animals [1–3]. Of various methods used for their removal from waters and wastewaters adsorption proves to be the most effective [4]. For this aim active carbons and biochars are successfully used.

Activated carbons (AC) are amorphous materials characterized by expanded surface area, porosity and availability of appropriate active centers which promotes absorption of gases and organic compounds. The main feedstock for the preparation of activated

* Corresponding author.
E-mail address: d.kolodynska@poczta.umcs.lublin.pl (D. Kołodyńska).

http://dx.doi.org/10.1016/j.cej.2016.08.088
1385-8947/

carbons is hard coal, due to its low production cost, good ion exchange properties and ease spent sorbents degradation [5]. The others include: peat, cellulose, fruit stones, nut shells, sugar cane etc. [6]. The type of feedstock as well as operating conditions of carbonization and activation processes affect physicochemical properties of activated carbons, their selectivity and capacity [5,7]. They are also widely used in: gas storage [8], catalysis [9], medicine and environmental protection [10].

Biochar (BC) is a carbon-rich solid product obtained by pyrolysis or gasification biomass in nitrogen atmosphere in the temperature range 623–1073 K. Properly selected gasification conditions such as temperature, vapour residence time, heating rate allow to control the properties of the resulting biochar [11,12]. Gasification allows for the reuse of agricultural solid wastes and wood, as well as refinery wastes. The thermochemical processes by which biomass can be converted are: slow pyrolysis, fast pyrolysis, flash carbonization, hydrothermal carbonization (HTC), gasification and torrefaction [13–18].

Gasification and hydrothermal carbonization are the two most efficient technologies to produce biochar. These methods are characterized by high efficiency and a wide range of materials. The HTC method consumes less energy because it does not require drying of biomass, such as slow pyrolysis [19]. As the optimal temperature for the production of biochar, Lehmann [12] indicates 823 K. This temperature allows to obtain good properties of biochar such as: cation exchange capacity, carbon content, surface area and porosity. Biochar obtained at low temperatures is characterized by a low adsorption capacity [20,21].

Suitable properties of biochar are decisive for its applications. In bioenergetics biochar is used as a renewable fuel [22,23]. The use of biochar for soil fertilization improves soil fertility by increasing pH. It is also used for long-term storage of carbon dioxide [24,25]. Biochar obtained from wastes provides a cheaper alternative to activated carbon and can be used to remove organic contaminants such as: hormones, dyes, pesticides, herbicids and inorganic impurities such as heavy metal ions from aqueous solutions and wastewaters [26,27]. There are numerous studies related to the sorption of heavy metal ions Cu(II), Cd(II), Zn(II), Pb(II), Cr(VI) using biochar obtained from: switchgrass, hardwood, corn straw etc. [28–30].

In the paper, the studies on sorption/desorption of heavy metals from the dairy manure-derived biochar (BC) produced by Coaltec Energy USA, Inc. and commercial active carbon (Purolite AC 20, denoted also as AC) were carried out. Special attention was paid to characterization of this new biosorbent (BC) and it was compared to the commercially activated carbon ion exchanger (AC). Kinetic and adsorption studies of Cu(II), Zn(II), Cd(II), Co(II) and Pb(II) were optimized and characterized. It is well known that desorption can be carried out using both mineral and organic acids. Therefore in the second stage desorption studies were performed and estimated. The washing method was applied using 0.1–1 M HNO_3, H_2SO_4 and HCl as eluents.

2. Materials and methods

2.1. Materials and their characterization

Biochar (denoted as BC) for testing was obtained from Coaltec Energy, USA Inc. This company has designed, patented and begun to deploy waste gasification systems in the USA and Europe on the commercial scale. The process is shown in Fig. 1. Gasification in the oxygen-free atmosphere allows to control formation of NO_x. The main product of gasification is CO with some methane and hydrogen contents. Then the synthesis gas is directed into the oxidizer where CO is oxidized to CO_2. Besides to biochar, a syngas mixture is formed during the gasification process. Biochar can be obtained from different fuels and animal manures through gasification. The material used for production of biochar and control of gasification parameters such as retention time and temperature, can affect the properties of biochar with respect to its application. Biochar is dry and pathogen-free and when added to the soil, it improves its fertility [31]. The physicochemical properties of biochar are presented in Table 1.

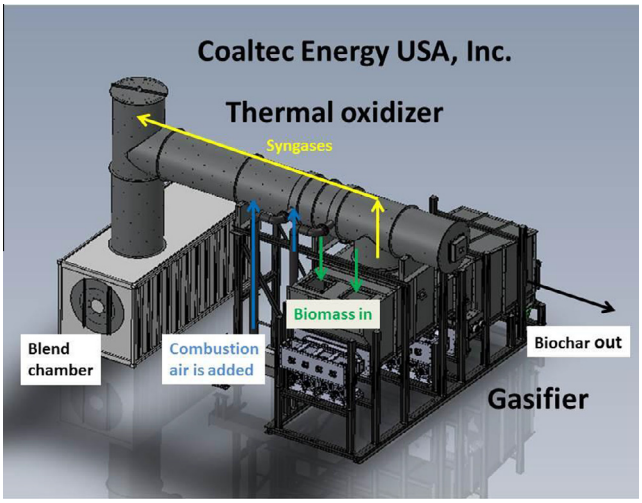

Fig. 1. Gasification process in Coaltec Energy USA, Inc.

Purolite AC 20 (denoted as AC) is a commercial activated carbon obtained from the bituminous coal mineral. Controlled thermal activation allows to obtain a high surface area and porous structure. Owing to its large resistance to abrasion, high density, short wetting time, as well as the sub-microscopic structure of its pores and their size, uniformly ranging from 1 to 100 nm it can be used as an effective sorbent. It is not only particularly suitable for the removal of chlorine, ozone and permanganate used in the pretreatment of potable waters, but also organic contaminants, heavy metals from waters and wastewaters. In addition, AC of large density has good resistance to the wearing and mechanical shocks [32].

Elemental analysis consisted in determining the percentage contents of carbon, hydrogen and nitrogen using a CHN analyzer 2400 Perkin-Elmer. The contents of moisture, ash and volatile compounds were determined using laboratory oven Thermolyne (Labo Plus, Thermo Scientific) in the temperature range 378–383 K, 1088 ± 283 K, 1123 ± 283 K, respectively.

The Fourier transform infrared spectroscopy (FT-IR) was used to analyze biochar and activated carbon before and after Cu(II) adsorption. It was achieved by means of Cary 630 FTIR

Table 1
Physicochemical characteristics of biochar and activated carbon.

Properties	BC	AC
Moisture content (%)	3.95	9.99
Ash content (%)	59.42	14.90
Volatile matter (%)	15.11	14.55
pH_{pzc}	9.8	6.8
%C	29.12	77.10
%H	0.82	1.41
%N	0.82	0.66
BET surface area (m^2/g)	115.5	759.9
Pore size (Å)[a]	58.763	55.789
Pore volume (cm^3/g)[b]	0.074724	0.420963

[a] Barrett, Joyner and Halenda (BJH) model, desorption data.
[b] $P/P_0 = 0.99$.

spectrometer (Agilent Technologies). The spectra were obtained in the range from 500 to 4000 cm^{-1}.

The morphology of sorbent surfaces was determined using a scanning electron microscope SEM (Tescan Vega, USA).

The measurements of average pore diameter, total pore volume and specific surface area were made by means of N_2 adsorption/desorption isotherms at 77 K using a porosimeter ASAP (Micromeritics, Inc. USA).

The thermogravimetric (TG) and derivative thermogravimetric (DTG) analyses for BC and AC were conducted using TA Instruments Q50 TGA. A test sample was heated at a constant rate of 283 K/min in the temperature range 298–1273 K. The measurements were performed in nitrogen atmosphere.

The pH of the point of zero charge pH_{pzc}, was measured by means of the pH drift method on a pH meter pHM82 (Radiometer, Copenhagen) [33].

2.2. Kinetic tests

$CuCl_2{\cdot}2H_2O$, $ZnCl_2$, $Cd(NO_3)_2{\cdot}4H_2O$, $CoCl_2{\cdot}6H_2O$ and $Pb(NO_3)_2$ were used as a source of metal ions. The stock solution was prepared by dissolving these salts in deionized water. The pH of solution was determined by adding 1 M HCl and 1 M NaOH. The solutions of HNO_3 H_2SO_4, HCl at various concentrations were used as the desorbing agents. All reagents were of analytical grade and were purchased from POCh (Poland).

The studies were carried out by the static method. The samples were shaken using the laboratory shaker type 358A (Elpin Plus, Poland). The pH was measured using a pH meter pHM82 (Radiometer, Copenhagen). Five stock solutions of 1000 mg/L Cu(II), Zn(II), Cd(II), Co(II) and Pb(II) were prepared by dissolving $CuCl_2{\cdot}2H_2O$, $ZnCl_2$, $Cd(NO_3)_2{\cdot}4H_2O$, $CoCl_2{\cdot}6H_2O$ and $Pb(NO_3)$ distilled water, respectively. They were further diluted in distilled water in order to obtain solutions with the concentrations: 50, 100, 150 and 200 mg/L. Adsorption was conducted in 100 mL conical flasks. The samples with a mass of 0.1 g of BC or AC and 20 mL of solution at a given concentration of heavy metal ions were shaken mechanically at 180 rpm at 293 K in the phase contact time from 1 to 360 min. The initial pH of the solutions was 5 and it was established by adding 1 M HCl or 1 M NaOH. After shaking, the solution was filtered. The concentration of Cu(II), Zn(II), Cd(II), Co(II), Pb(II) in solution was determined by atomic absorption (AAS) at 324.7 nm for Cu (II), 213.9 nm for Zn(II), 228.8 nm for Cd(II), 240.7 nm for Co(II), and 217.0 nm for Pb(II).

2.3. Desorption studies

Desorption study was carried out in a similar way to that of sorption studies. After sorption metal-loaded BC and AC (initial concentration of metal ions 200 mg/L, pH 5, shaking speed 180 rpm, temperature 295 K) were dried, weighed and shaken with 20 mL of eluents in 100 mL conical flasks at 180 rpm on a laboratory shaker. As eluents HNO_3, H_2SO_4 and HCl of different concentrations 0.1 M, 0.5 M and 1 M were used.

2.4. Calculations

The amount of adsorbed heavy metal ions q_t (mg/g) and the sorption percentage %S (%) were calculated according to:

$$q_t = \frac{(C_0 - C_t)V}{m} \quad (1)$$

$$\%S = \frac{(C_0 - C_t)}{C_0} 100\% \quad (2)$$

where: V (L) is the volume of solution, m (g) is the mass of sorbent and C_0 and C_t (mg/L) are the initial concentrations and those of metal ions after time t in the solutions, respectively.

In order to investigate the mechanism of adsorption of: Cu(II), Zn(II), Cd(II), Co(II), Pb(II) ions on BC and AC there were used pseudo first order (PFO) and pseudo second order (PFO) equations. The pseudo first order kinetic equation is represented by Eq. (3) [34]:

$$\log(q_1 - q_t) = \log(q_1) - \frac{k_1 t}{2,303} \quad (3)$$

The pseudo second order (PSO) kinetic equation is represented by Eq. (4) [35]:

$$\frac{t}{q_t} = \frac{1}{k_2 q_2^2} + \frac{t}{q_2} \quad (4)$$

and the intraparticle diffusion model (IPD) is expressed as Eq. (5) [36]:

$$q_t = k_i t^{1/2} + C \quad (5)$$

where: k_1 is the rate constant of the pseudo first order sorption (1/min), k_2 is the pseudo second order rate constant (g/mg min), k_i is the rate constant of the intraparticle diffusion (mg/g $min^{0.5}$) and C is the intercept which reflects the boundary layer effect.

The desorption percentage (%) was determined using Eq. (6):

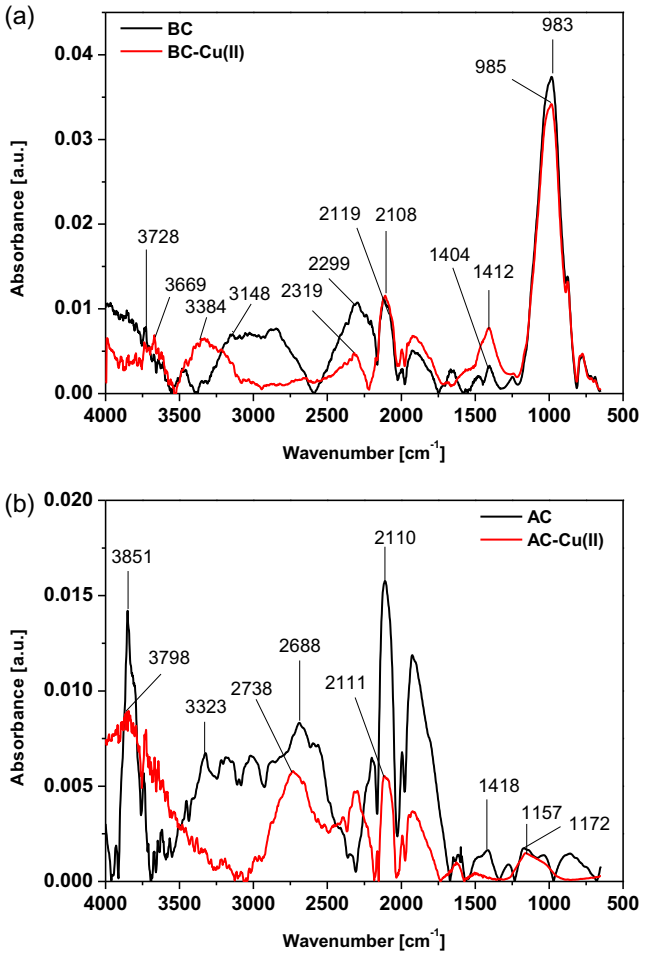

Fig. 2a–b. FT-IR spectra of BC (a) and AC (b) before and after the reaction with 200 mg/dm^3 Cu(II) for 6 h at pH 5.

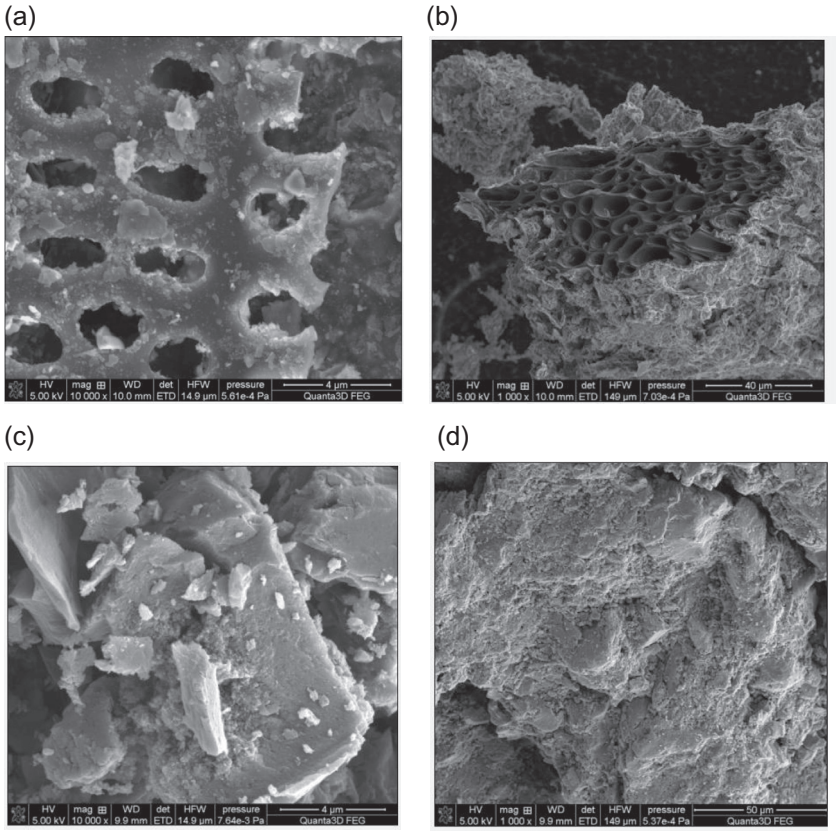

Fig. 3a–d. SEM images of BC sample at (a) 10,000× and (b) 1000× magnifications and AC sample at (c) 10,000× and (d) 1000× magnifications.

$$\%D = \frac{C_{des}}{C_0} \times 100\% \quad (6)$$

where: C_{des} (mg/L) is the concentration of metal ions in solution after desorption.

The content of ions Cu(II), Zn(II), Cd(II), Co(II), Pb(II) in the solution was determined using atomic absorption spectrometer AAS (Spectr AA 240 FS, Varian) which was equipped with a background correction, deuterium lamp, cathode lamp for Cu, Zn, Cd, Co, Pb and an air-acetylene burner.

3. Results and discussion

3.1. Physicochemical characterization of BC and AC

In Table 1 the physicochemical properties of BC and AC are shown. The contents of remaining C, H and N for BC are: 29.12%, 0.82%, 0.82% and for AC: 77.10%, 1.41%, 0.66%, respectively. The contents of these elements are higher for AC than BC. The molar ratios of H/C for BC and AC are 0.34 and 0.22, respectively. Carbon sorbents are characterized by strong carbonization and high aromaticity if the molar ratio of H/C is less than 0.5 [37,38]. The moisture content of AC equal to 9.99% is higher than that for BC 3.95%. The ash content of BC is high and equal to 59.42%, as for AC it is lower and equal to 14.90%. The ash content of biochar determines the possibility of its use for agricultural purposes. Since the higher ash content of the more essential nutrients affects plant growth [39]. It was found that the volatile matter is 15.11% for BC and 14.55% at for AC.

Fig. 2a–b. shows the FTIR spectra of BC (a) and AC (b) before and after Cu(II) sorption in order to determine the change in the oscillation frequency of functional groups. The IR spectra indicate the complex nature of BC and AC. The bands at 3728 cm^{-1} and 3148 cm^{-1} before and at 3669 cm^{-1} and 3384 cm^{-1} after sorption were assigned to O–H stretching vibration of BC and at 3851 cm^{-1} and 3323 cm^{-1} before sorption and at 3798 cm^{-1} for AC after sorption [40,41]. The peaks at 2688 cm^{-1} before and at 2735 cm^{-1} after sorption in AC can be assigned to –CH stretching vibrations [42]. The bands in the range 2000–2500 cm^{-1} are assigned to C≡C and –C≡N triple bonds or accumulated in C=C=C– and –N=C=O double bonds [38]. The peaks which are representatives of aromatic C=O and C=C functional groups occur at 1404 cm^{-1} before and at 1412 cm^{-1} after sorption of Cu(II) on BC and at 1418 cm^{-1} before sorption on AC [39]. The bands at 1172 cm^{-1} and 1157 cm^{-1} corresponded to CO– stretching in alcohols and phenols in AC before and after sorption, respectively [43]. Strong peaks at 983 cm^{-1} and 985 cm^{-1} are assigned to aromatic ring in BC before and after sorption, respectively [44]. The resulting spectra are similar to those in [39,40,42,44]. The bands at 3323 cm^{-1} and 1418 cm^{-1} in AC responsible for O–H stretching and C=O groups disappear after Cu(II) sorption. Therefore it can be stated that carboxyl and hydroxyl groups take part in sorption of Cu(II) ions [42]. For BC it was also shown that the band connected with –OH groups shifts from 3148 cm^{-1} to 3384 cm^{-1} after the sorption process. This observation may indicate a complex structure of biochar with phenolic groups on the surface during sorption [45].

In Fig. 3a–d. the SEM images of BC and AC samples at two different magnifications are presented. It can be argued that both sorbents have a heterogeneous, well-developed structure [29,46]. Additionally, according to the SEM-EDX analysis the sorbed heavy metal ions are uniformly distributed on the surface and interior of BC and AC sorbents and they are characterized by a smoother, compact and uniform structure.

The specific surface area is smaller for BC 115.5 m^2/g than for AC 759.8 m^2/g. The measured values of surface area, pore size and pore volume are listed in Table 1. The N_2 adsorption/desorption isotherms (Fig. 4a–b) of BC resemble the Type IV isotherm and H3 hysteresis loop according to the IUPAC classification. The hysteresis loop suggests the presence of mesopores (pores of the width 20–500 Å) between the slits of the micropores and the possibility of capillary condensation in the pores [30]. The N_2 adsorption/desorption isotherms of AC can resemble the Type I isotherm with tendency to form a plateau at low relative pressures and predominance of micropores in the sorbent. After filling the micropores N_2 adsorption is likely to continue in the mesopores [47,48]. In Fig. 5a–b. the pore size distribution of BC and AC obtained from N_2 desorption isotherm curves is presented. The pore distribution curves are in the range of micropores [49].

Point of zero charge (pH_{pzc}) was determined with a graph of ΔpH (pH_1–pH_0) vs. pH_0 (Fig. 6a–b). For BC pH_{zpc} is equal to 9.8 whereas for AC this value is 6.8. When the pH is less than pH_{zpc} the surface of the sorbent is positively charged which increases the electrostatic repulsion between the sorbent surface and heavy metal ions. Negatively charged surface is formed when the pH is greater than pH_{zpc}. Then the attraction increases between the sorbent surface and the Cu(II), Zn(II), Cd(II), Co(II) and Pb(II) ions. Mohan et al. noted that at low pH increases the equilibrium pH of the solution vs. the initial pH. As a result, it increases the sorption capacity of the sorbent. pH 5 is indicated as the optimum pH sorption [50]. On the surface of BC and AC negatively charged functional groups are present that attract heavy metal cations.

However, the sorption process of metal ions is very complex. As follows from the literature data the carboxyl (–COOH), hydroxyl (–OH), phenol (R–OH) groups are generally accepted as the main groups contributing to coordination of heavy metal ions such as Cu(II), Zn(II), Cd(II), Co(II) and Pb(II) etc. on the sorbent surface. Complexation of metals with these ionized oxygen-containing functional groups through ion exchange has been suggested as a major mechanism for metal sorption by biochar. As the hydroxyl and carboxylic groups on biochars surface became deprotonated (COO^- and $-O^-$) at the wide pH range, the formation of $-(COO)_2M$, $-COOM^+$ and $-(O)_2M$, $-OM^+$ as well as $-(RO)_2M$ occurs as presented below:

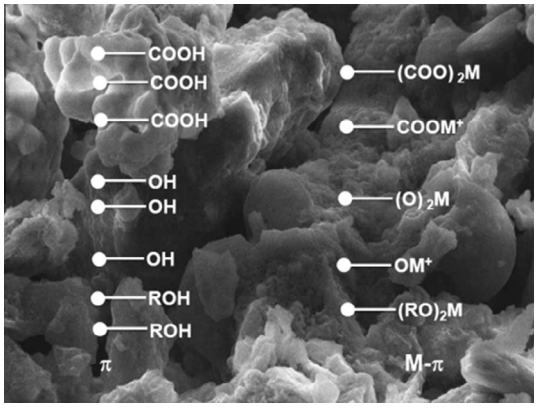

It is also well known that as the pyrolysis temperature increased, more aromatic structures are formed in the biochar due to the high degree of graphitization. They can act as π donors in metal ions sorption process. The precipitation process should also be taken into account.

In Fig. 7a–b. the TG and DTG curves are compared. From the TG curve analysis of BC and AC (% weight loss dependence on the temperature), it was found that BC is more stable than AC at low temperatures. The DTG curves show the rate of weight loss at a particular temperature. It was found that the weight loss for AC is mainly observed at temperatures up to 373 K, however, for BC in the range 873–973 K [37]. This is due to the thermal decomposition of aromatic hydrocarbons and carbonates in the sample of BC [51].

3.2. Effect of initial concentrations of metal ions and phase contact time

The adsorption efficiency of BC is higher than that of AC. This is because that the adsorption of heavy metal ions on biochar is not related to the nature of its surface [37]. The improvement of metal sorption by biochars is associated with the origin of the material and for well-developed biochars it is greater for Pb(II).

The sorption process of Cu(II), Zn(II), Cd(II), Co(II) and Pb(II) on BC and AC was tested at a different phase contact times (1–360 min.), at different initial concentrations of metal ions (50–200 mg/L) and at 295 K and pH 5. The pH effect on the sorption yield was not determined because it was reported in [11]. Under acidic conditions, the groups on the BC surface are protonated, however, at higher pH values the carboxyl groups become deprotonated which affects the metal ions sorption. The same situation is observed for AC. Therefore it can be assumed that the optimal pH value for the most efficient removal of metal ions by BC and AC is at pH above 5.0.

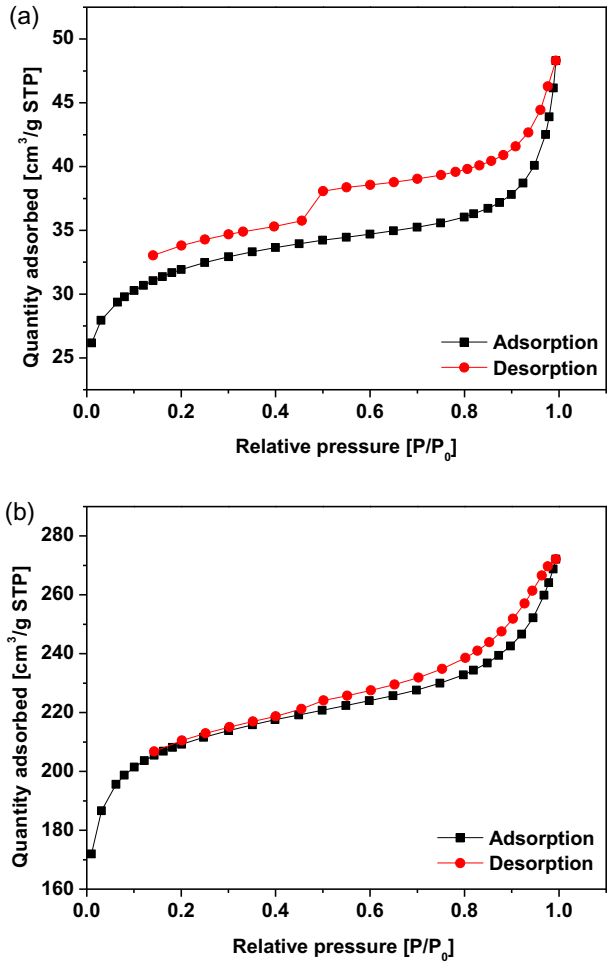

Fig. 4a–b. N_2 adsorption and desorption isotherms at 77 K of BC (a) and AC (b).

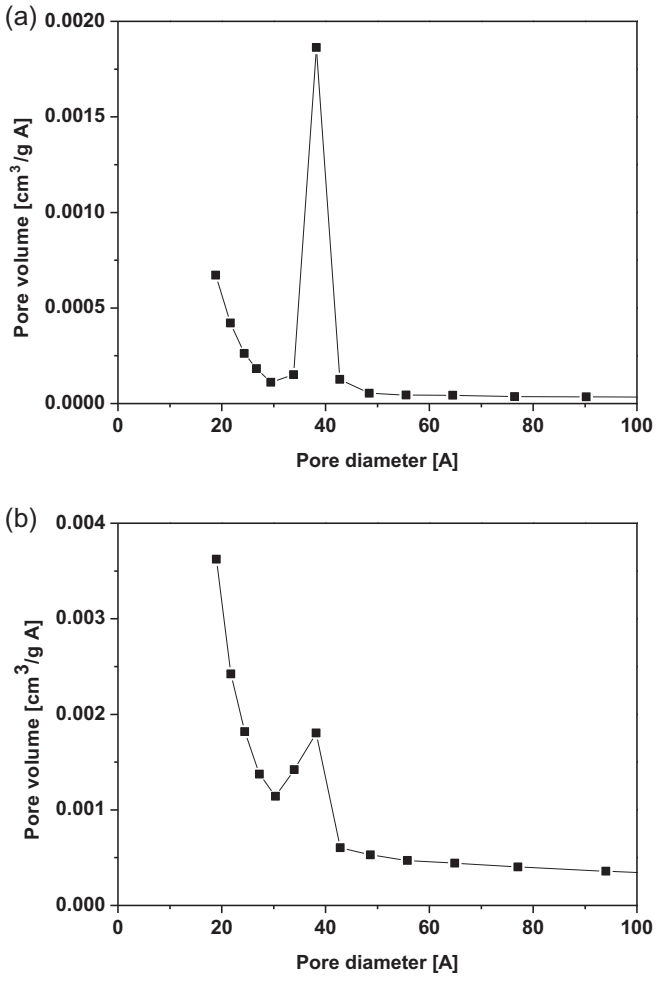

Fig. 5a–b. Pore size distribution of (a) BC and (b) AC.

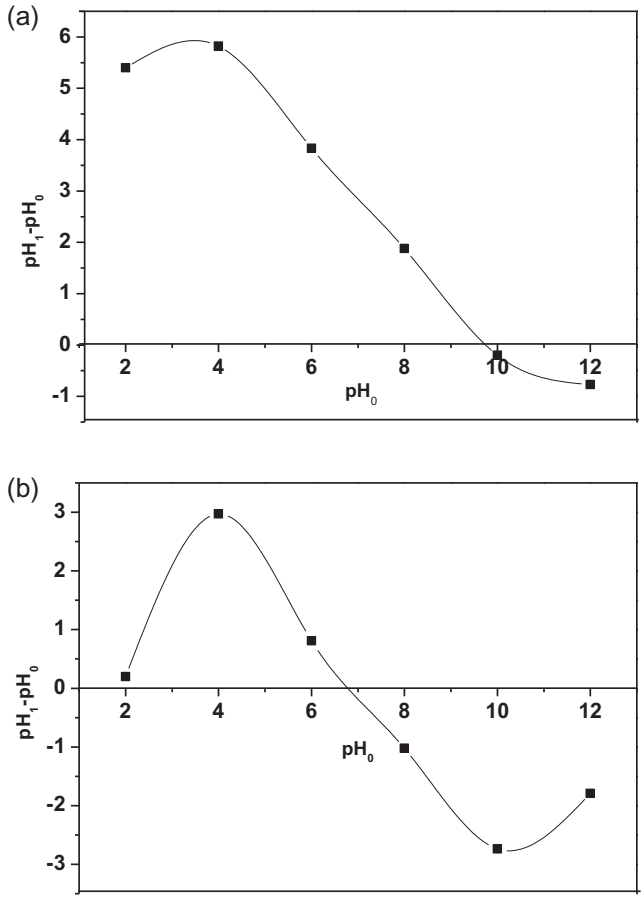

Fig. 6a–b. Point of zero charge of (a) BC and (b) AC.

It was noted that the sorption capacity increases with the increasing phase contact time and initial concentration of the solution. It was found that for Cu(II) the plateau was established at 9.98 mg/g, 19.42 mg/g, 22.93 mg/g, 24.95 mg/g sorption on BC and 4.62 mg/g, 6.36 mg/g, 8.16 mg/g, 8.47 mg/g sorption on AC at the concentrations 50, 100, 150, 200 mg/L, respectively. For the other heavy metal ions the same relationships were found. The equilibrium time is independent of initial concentration. Moreover, sorption by BC and AC showed the same shape, characterized by a sharp increase of the capacity during the first minutes of contact between the solution and solid phases, followed by a slow increase. It can be estimated that fast diffusion onto the external surface is followed by slow pore diffusion. The results for the Cu(II) adsorption on BC and AC is presented in Fig. 8a–b. For Zn(II), Cd(II), Co (II) and Pb(II) ions sorption on BC and AC are shown in Fig. S1. Similar results were obtained by Li et al. [52] in the case of the adsorption of Cu(II) on biochar derived to *Spartina alterniflora*. The sorption capacity increases from 9.10 mg/g for the concentration of the initial solution of 50 mg/L to 49.14 mg/g for the concentration of 290 mg/L. The sorption capacity for the initial concentration of 200 mg/L was 23.26 mg/g for Zn(II), 33.90 mg/g for Cd(II), 20.23 mg/g for Co(II) and 37.80 mg/g for Pb(II) sorption on BC and 12.90 mg/g, 12.64 mg/g, 6.90 mg/g and 29.20 mg/g sorption on AC, respectively. It was found that S% decreases with the increasing concentration of the initial solution of Co(II) in the range 50–200 mg/L from 79.68% to 50.57% for BC and from 46.17–17.25% for AC. For the remaining heavy metal ions the same relationship was observed. Similar results were obtained by Vilvanathan et al. [53] in the case of investigating the adsorption of Co(II) on biochar of *Chrysanthemum indicum* flower. S% decreases from 99.48–62.37% with the increasing initial concentration from 25 to 200 mg/L. Comparing the sorption capacity it can be concluded that BC removes more efficiently heavy metal ions from aqueous solutions than AC. The highest value q_t was obtained for the sorption of Pb(II) on biochar.

3.3. Adsorption kinetics

The kinetics of sorption of heavy metal ions depends on the physical and/or chemical properties of BC and AC [11]. To determine the adsorption kinetics three models were used: the pseudo first order (PFO) proposed by Lagergren, the pseudo second order (PSO) used by Ho and McKay and the intraparticle diffusion model (IPD) by Weber and Morris [34–36]. In Tables 2 and 3 the kinetic parameters of metal ions sorption process on BC and AC were collected. It can be concluded that the best fit of the experimental data is exhibited by the PSO model in which the determination coefficient (R^2) is higher than 0.91 and the values predicted from the experimental data q_2 and q_{exp} are almost equal. This model is based on the assumption that the rate limiting stage can be a chemical adsorption involving valence forces through sharing or exchange of electrons between adsorbent and adsorbate. The low values of rate constant (k_2) suggested that the adsorption rate decreased with the increase of the phase contact time and the adsorption rate was proportional to the number of unoccupied sites. Ding et al. obtained similar results studying the adsorption of Pb(II) on the bagasse biochar [54].

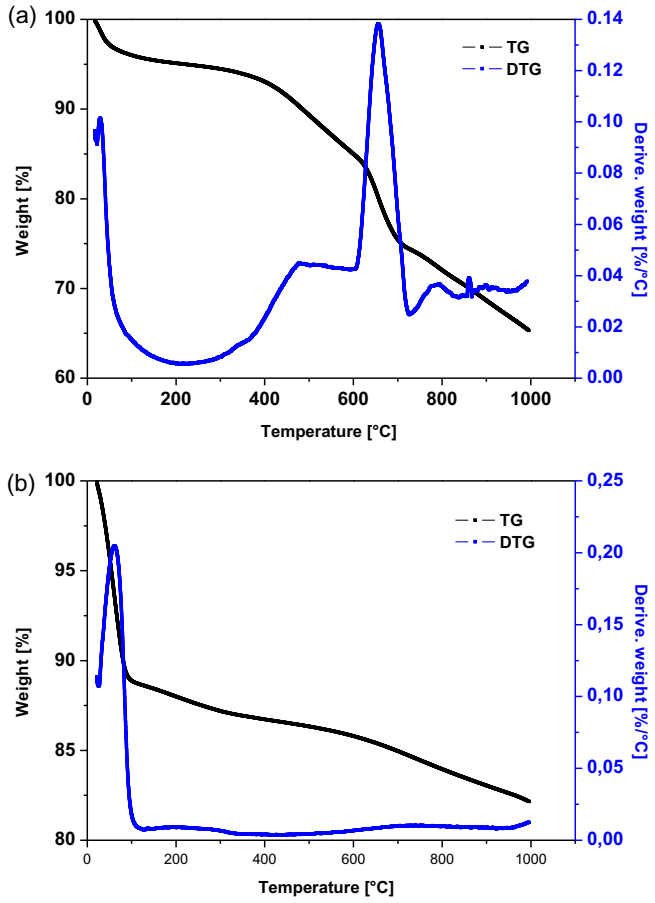

Fig. 7a–b. TG and DTG curves of BC (a) and AC (b).

The kinetic metal ions sorption and rates of sorption on BC follow this order: Pb(II) > Cd(II) > Cu(II) > Zn(II) > Co(II) and on AC follow this order: Pb(II) > Zn(II) > Cd(II) > Cu(II) > Co(II). The mechanisms of sorption of heavy metal ions can be explained by the two adsorption processes: physical adsorption and chemisorption.

Table 4 shows the comparison of adsorption of heavy metal ions by different BC and AC. The detail summarizes of adsorptions of different species on various biochar types are presented in [26]. It can be observed that in many cases the AC exhibited much higher removal capacity than that shown by BC. Higher adsorption capacities of AC are attributed to several factors, including the physicochemical properties (high specific surface area, pore size, type of the functional groups), high affinity etc.

3.4. Desorption studies

Adsorption and desorption properties indicate usability of the sorbent. It is important that the sorbent is easily regenerated and the desorbing agent are effective, cheap, non-polluting and non-damaging the structure of the sorbent [58,59].

The regeneration of the adsorbents was achieved by washing loaded sorbents with different desorbing agents: HNO_3, H_2SO_4, HCl at different concentrations 0.1 M, 0.5 M and 1 M. In order to determine the time at which the highest percentage of desorption (D%) can be achieved for BC and AC, the phase contact time in the range 15–480 min. was applied. In the studies the desorbing agent 0.1 M HNO_3 was used. Metal concentration was determined in the samples removed after 15, 30, 60, 120, 180, 240, 300, 360, 480 min. (Fig. 9a–b). In order to investigate the effect of various factors the desorption process was carried out at 360 min after which equilibrium was noted.

Fig. 10a–b. shows the desorption efficiency of Cu(II), Zn(II), Cd (II), Co(II) and Pb(II) using 0.1 M HNO_3. Fig. S2 presents the desorption efficiency using H_2SO_4 and HCl under the same conditions. Of all analyzed elements Cd(II) adsorbed on the BC displayed the most effective removal of 1 M solutions of acids, with the efficiency 96.86% for HNO_3, 98.58% for H_2SO_4 and 97.15% for HCl. Nitric(V) acid showed the best removal of Cu(II) adsorbed on AC with the efficiency 80.58%, sulfuric acid(VI) preferably removed Cd(II) with efficiency 60.08%, hydrochloric acid preferably removed Zn(II) with the efficiency 56.48% (for acids at a concentration of 1 M). Similar results were obtained in [12]. The highest removal efficiency of metal ions was observed for 3.5 M HNO_3 and the removal percentages of Cd(II), Cu(II) and Zn(II) ions were equal to 91%, 95%, and 93%, respectively. However, higher acid concentration may damage the BC structure and reduce the sorption and desorption efficiency due to a biosorbent mass loss. When HCl acid was used, the maximal desorption efficiencies were obtained for higher concentrations e.g. 6 M for Zn(II) and 9.5 M for Cd(II) and Cu(II), which gave desorption values of 90%, 90%, and 85%, respectively.

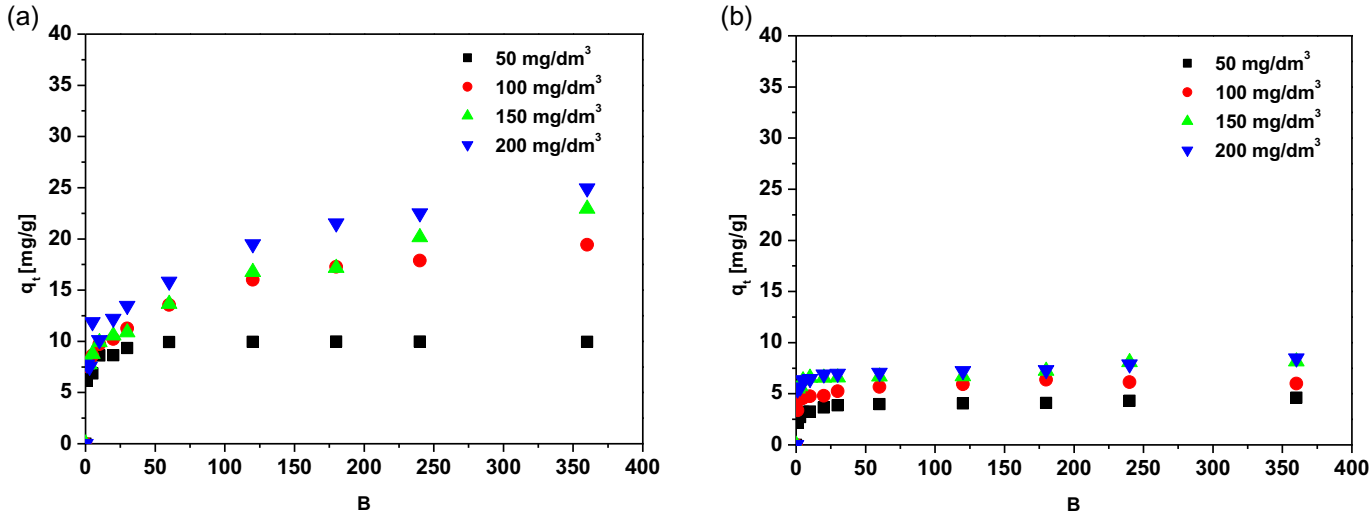

Fig. 8a–b. Effect of the phase contact time on Cu(II) adsorption on BC (a) and AC (b) for different metal ion concentrations (pH 5, shaking speed 180 rpm, temperature 295 K).

Table 2
Kinetic parameters for Cu(II), Zn(II), Cd(II), Co(II) and Pb(II) on BC.

c_0	q_{exp}	PFO			PSO				IPD		
		q_1	k_1	R^2	q_2	k_2	h	R^2	k_i	C	R^2
Cu(II)											
50 mg/dm^3	9.98	2.23	0.036	0.898	10.02	0.067	6.638	1.000	0.307	5.893	0.445
100 mg/dm^3	19.42	10.94	0.009	0.988	19.42	0.004	1.371	0.993	0.818	5.838	0.860
150 mg/dm^3	22.93	14.59	0.006	0.968	22.37	0.002	1.108	0.975	0.959	5.416	0.911
200 mg/dm^3	24.95	15.48	0.008	0.983	24.88	0.002	1.408	0.989	1.099	6.190	0.896
Zn(II)											
50 mg/dm^3	9.59	2.50	0.008	0.699	9.51	0.023	2.160	0.998	0.290	5.245	0.495
100 mg/dm^3	18.57	9.63	0.012	0.940	18.87	0.005	1.575	0.995	0.747	6.737	0.787
150 mg/dm^3	20.78	5.58	0.006	0.889	20.37	0.009	3.731	0.997	0.583	11.428	0.468
200 mg/dm^3	23.26	9.95	0.007	0.796	22.73	0.005	2.647	0.994	0.888	8.861	0.730
Cd(II)											
50 mg/dm^3	9.91	3.96	0.033	0.964	9.95	0.032	3.141	1.000	0.335	5.213	0.550
100 mg/dm^3	19.74	9.45	0.019	0.991	20.08	0.007	2.771	0.999	0.738	8.761	0.692
150 mg/dm^3	28.30	13.96	0.012	0.983	27.25	0.005	4.134	0.995	1.991	5.617	0.836
200 mg/dm^3	33.90	19.95	0.013	0.970	34.48	0.002	2.513	0.993	1.450	10.769	0.831
Co(II)											
50 mg/dm^3	7.97	3.40	0.017	0.983	8.00	0.020	1.289	0.999	0.286	3.684	0.654
100 mg/dm^3	14.16	7.00	0.007	0.948	13.83	0.006	1.125	0.988	0.533	4.983	0.783
150 mg/dm^3	16.60	6.14	0.008	0.788	16.34	0.007	2.030	0.995	0.539	7.740	0.539
200 mg/dm^3	20.23	9.07	0.008	0.957	19.96	0.004	1.691	0.988	0.696	8.276	0.696
Pb(II)											
50 mg/dm^3	9.96	10.98	0.015	0.540	9.97	0.811	80.558	1.000	0.187	7.654	0.170
100 mg/dm^3	19.86	7.31	0.028	0.635	19.84	1.155	455.56	1.000	0.338	15.728	0.138
150 mg/dm^3	28.67	4.20	0.012	0.569	28.74	1.730	1421.99	1.000	0.511	22.437	0.152
200 mg/dm^3	37.80	3.86	0.014	0.767	37.88	0.027	38.163	1.000	0.939	25.469	0.308

Table 3
Kinetic parameters for Cu(II), Zn(II), Cd(II), Co(II) and Pb(II) on AC.

c_0	q_{exp}	PFO			PSO				IPD		
		q_1	k_1	R^2	q_2	k_2	h	R^2	k_i	C	R^2
Cu(II)											
50 mg/dm^3	4.62	1.42	0.007	0.766	4.52	0.038	0.809	0.997	0.150	2.269	0.558
100 mg/dm^3	6.36	2.03	0.014	0.890	6.12	0.069	2.786	1.000	0.198	3.373	0.510
150 mg/dm^3	8.16	2.03	0.004	0.698	8.08	0.019	1.241	0.994	0.221	4.613	0.436
200 mg/dm^3	8.47	2.19	0.004	0.632	8.24	0.020	1.436	0.995	0.231	4.680	0.445
Zn(II)											
50 mg/dm^3	4.75	1.04	0.004	0.914	4.63	0.042	0.950	0.996	0.110	2.932	0.326
100 mg/dm^3	8.48	1.32	0.008	0.655	8.40	0.049	3.504	0.999	0.278	5.373	0.350
150 mg/dm^3	9.92	2.24	0.012	0.510	9.85	0.040	3.959	0.999	0.302	5.671	0.449
200 mg/dm^3	12.90	10.41	0.025	0.776	12.69	0.005	0.885	0.986	0.681	2.278	0.804
Cd(II)											
50 mg/dm^3	5.35	1.67	0.006	0.812	5.25	0.132	3.776	1.000	0.110	3.761	0.227
100 mg/dm^3	10.47	1.96	0.012	0.815	9.55	0.062	6.798	0.994	0.247	6.659	0.304
150 mg/dm^3	12.37	7.72	0.042	0.888	12.21	0.013	1.962	0.997	0.516	4.733	0.572
200 mg/dm^3	12.64	7.60	0.033	0.881	13.59	0.003	0.483	0.916	0.629	3.741	0.664
Co(II)											
50 mg/dm^3	4.64	1.84	0.016	0.960	4.66	0.038	0.827	0.999	0.168	2.173	0.638
100 mg/dm^3	5.47	1.13	0.006	0.867	5.38	0.041	1.231	0.998	0.137	3.335	0.364
150 mg/dm^3	6.45	1.95	0.021	0.848	6.01	0.262	10.91	0.995	0.415	2.231	0.672
200 mg/dm^3	6.90	1.69	0.013	0.974	6.91	0.040	1.902	0.999	0.193	4.102	0.429
Pb(II)											
50 mg/dm^3	8.67	1.53	0.007	0.760	8.58	0.032	2.373	0.999	0.208	5.515	0.322
100 mg/dm^3	16.38	4.18	0.012	0.622	16.03	0.025	6.616	0.999	0.525	8.746	0.503
150 mg/dm^3	20.72	4.87	0.011	0.688	20.62	0.013	5.626	0.999	0.570	12.303	0.420
200 mg/dm^3	29.20	9.17	0.004	0.962	27.40	0.005	3.917	0.984	0.788	14.800	0.474

In Fig. 11a–b the desorption efficiency using HNO_3, H_2SO_4 and HCl at a concentration 0.1 M is presented. The use of acids exhibits similar desorption efficiency of metal ions from BC and AC. A slightly higher efficiency is exhibited by 0.1 M HNO_3. These acids can be used as desorbing agents. Under acidic conditions the surface of the sorbent is protonated which allows desorption of positively charged ions [60]. Because of the low solubility of the lead sulfate, H_2SO_4 should not be used for recovery of Pb (II). Such conditions result in the surface precipitation of metal ions which in combination with the lower pore volume of BC prevents complete desorption. Therefore, it can be concluded that HNO_3 is the best eluent. With the increase in the acids

Table 4
Sorption capacities of AC and BC for Cu(II), Zn(II), Cd(II), Pb(II) and Co(II).

Adsorbent	Ion	Max. sorption capacity [mg/g]	Parameters	Reference
OG-AC 9 outgassed activated carbon)	Cd(II)	–	pH ranged 5.6–6.1 for OG-AC	[55]
OG-AC 9 outgassed activated carbon)	Zn(II)	8.69 mg/g	pH ranged 5.6–6.1 for OG-AC	[55]
Mg-AC (magnesium and activated carbon composite)	Cd(II)	10.56 mg/g	pH ranged 5.5–5.9 for Mg-AC	[55]
Mg-AC (magnesium and activated carbon composite)	Zn(II)	9.68 mg/g	pH ranged 5.5–5.9 for Mg-AC	[55]
PHHC (peanut hull hydrochar)	Pb(II)	0.88 mg/g	n.a.	[56]
mPPHC (after modification using 10% H_2O_2 solution for 2 h at 295 K)		22.82 mg/g	n.a.	[56]
Pinewood BC	Pb(II)	4.25 mg/g	n.a.	[57]
Rice husk BC	Pb(II)	2.4 mg/g	n.a.	[57]

n.a. not available.

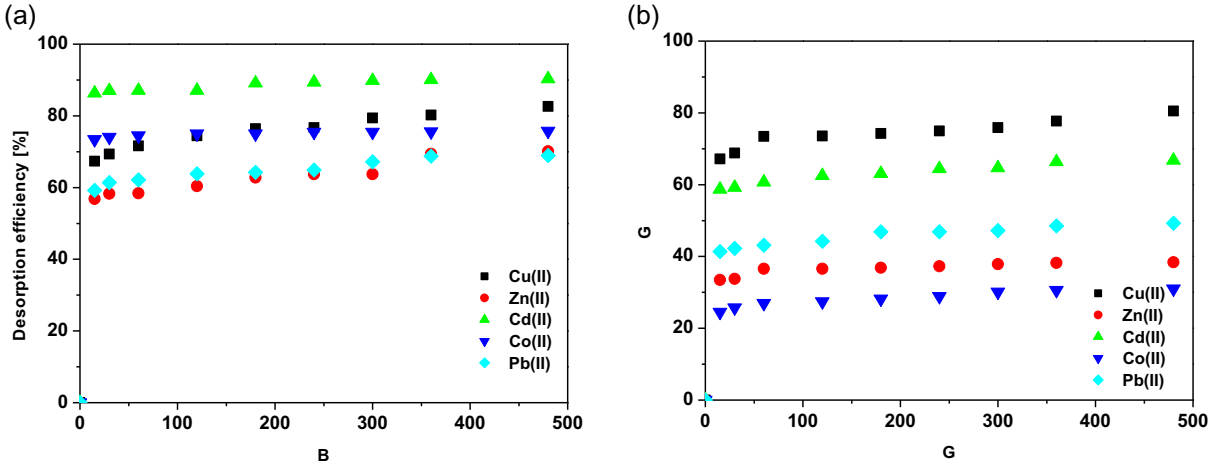

Fig. 9a–b. Elution of Cu(II), Zn(II), Cd(II), Co(II) and Pb(II) from metal-loaded BC (a) and AC (b) using 0.1 M HNO_3.

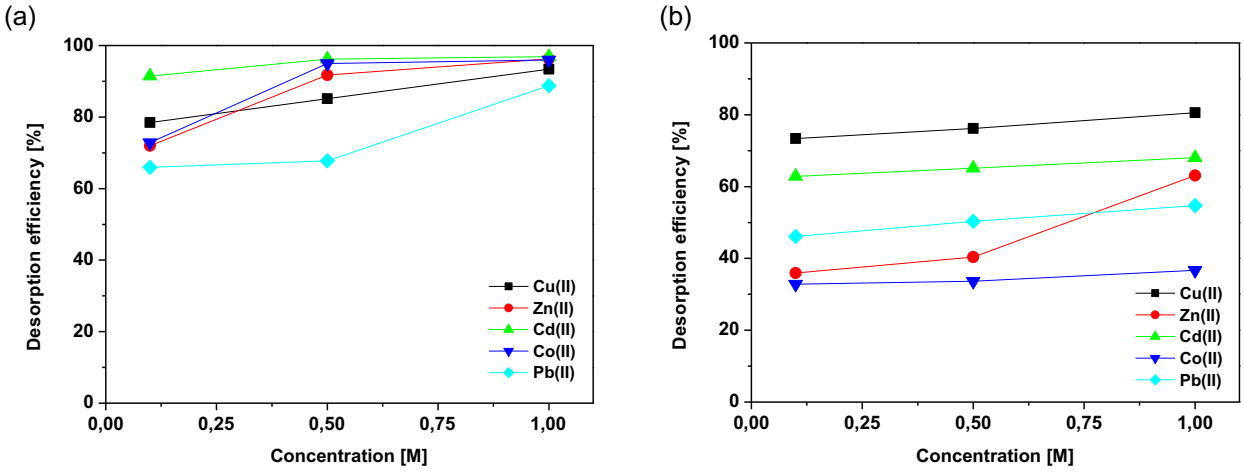

Fig. 10a–b. Comparison between Cu(II), Zn(II), Co(II), Cd(II) and Pb(II) elution from metal loaded BC (a) and AC (b) using different concentrations of HNO_3.

concentration, the desorption efficiency increases. Acid solutions were used in the concentration range 0.1–1 M since higher concentrations could damage the structure of the sorbent for both BC and AC. The results show that BC is easier to regenerate than AC.

The metal-desorbed BC and AC were used as the regenerated sorbent in three sorption/desorption cycles. However, no significant change in the sorption/desorption efficiency was observed (Fig. 12). Therefore, they can be infinitely reused in acid treatment without losing their adsorption capacity.

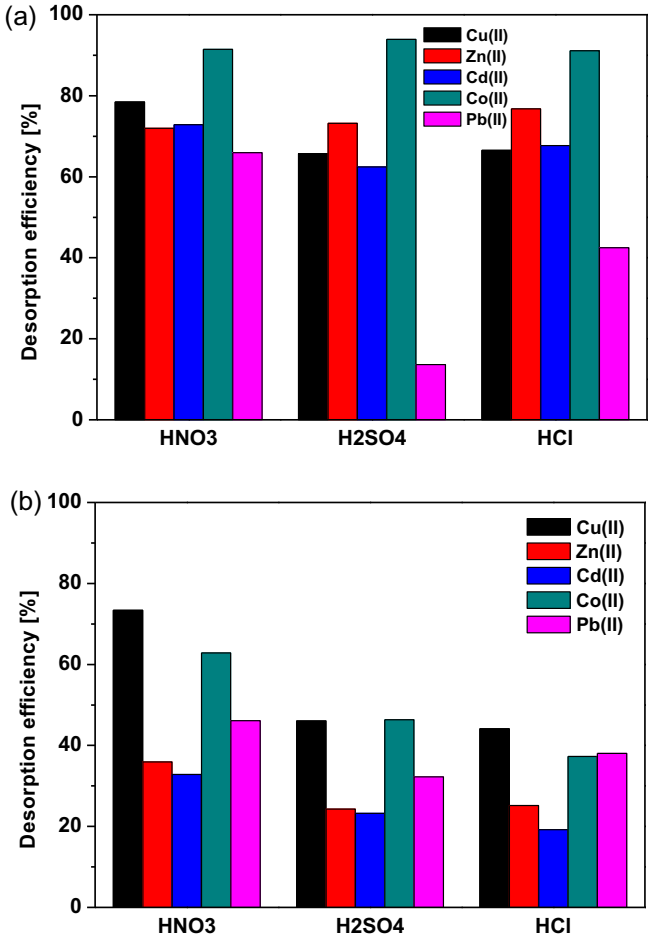

Fig. 11a–b. Comparison between Cu(II), Zn(II), Co(II), Cd(II) and Pb(II) elution from metal-loaded BC (a) and AC (b) using different desorbing agents at a concentrations of 0.1 M.

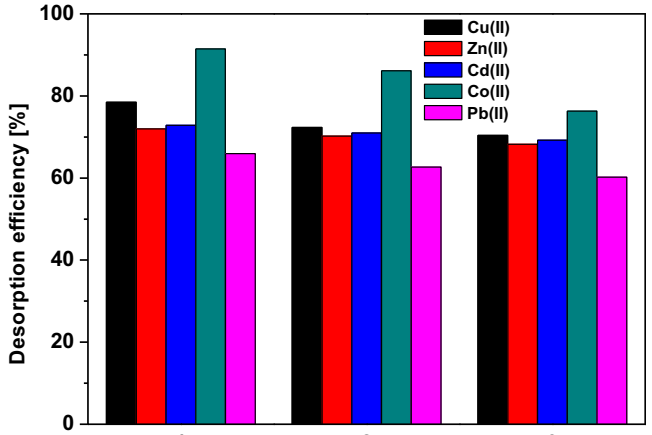

Fig. 12. Comparison of between Cu(II), Zn(II), Co(II), Cd(II) and Pb(II) elution from metal-loaded BC using 0.1 M HNO_3 in three sorption–desorption cycles.

4. Conclusions

1) Biochar (BC) and commercial active carbon (AC) were compared as far as sorption and desorption of Cu(II), Zn(II), Cd (II), Co(II) and Pb(II) ions from aqueous solutions.
2) For both sorption capacity increases with the increasing phase contact time and initial concentration of metal ions.
3) BC shows an increase in adsorption activity with respect to Pb(II) > Cd(II) > Cu(II) > Zn(II) > Co(II) ions in comparison with the initial AC. The highest adsorption capacity for BC was found at pH 5.0 to be equal 37.80 mg/g for Pb(II), 33.90 mg/g for Cd(II), 24.95 mg/g for Cu(II), 23.26 mg/g for Zn(II) and 20.23 mg/g for Co(II). For AC these values were lower.
4) The kinetic parameters (R^2, q_2) show the best fit for the PSO model and provide a complex mechanism of sorption.
5) It was shown that both sorbents can be regenerated in solutions of acids of which HNO_3 is the most effective. It was found that 88.79% of Pb(II), 96.88% of Cd(II), 96.23% of Zn (II), 93.38% of Cu(II) and 95.96% of Co(II) ions leached from BC in acidic solutions, while only 54.69% of Pb(II), 68.08% of Cd(II), 63.08% of Zn(II), 80.58% of Cu(II) and 36.70% of Co (II) ions can be removed from AC.

Appendix A. Supplementary data

Supplementary data associated with this article can be found, in the online version, at http://dx.doi.org/10.1016/j.cej.2016.08.088.

References

[1] F.M. Pallera, A. Giannis, D. Kalderis, K. Anastasiadou, R. Stegmann, J.Y. Wang, E. Gidarakos, Adsorption of Cu(II) ions from aqueous solutions on biochars prepared from agricultural by-products, J. Environ. Manage. 96 (2012) 35–42.
[2] Z. Song, F. Lian, Z. Yu, L. Zhu, B. Xing, W. Qiu, Synthesis and characterization of a novel MnO_x-loaded biochar and its adsorption properties for Cu^{2+} in aqueous solution, Chem. Eng. J. 242 (2014) 36–42.
[3] M. Schwamborn, Chemical synthesis of polyaspartates: a biodegradable alternative to currently used polycarboxylate homo- and copolymers, Polym. Degrad. Stab. 59 (1998) 39–45.
[4] M. Karnib, A. Kabbani, H. Holail, Z. Olama, Heavy metals removal using activated carbon, silica and silica activated carbon composite, Energy Procedia 50 (2014) 113–120.
[5] S.F. Lo, S.Y. Wang, M.J. Tsai, L.D. Lin, Adsorption capacity and removal efficiency of heavy metal ions by Moso and Ma bamboo activated carbons, Chem. Eng. Res. Des. 90 (2012) 1397–1406.
[6] H. Treviño-Cordero, L.G. Juárez-Aguilar, D.I. Mendoza-Castillo, V. Hernández-Montoya, A. Bonilla-Petriciolet, M.A. Montes-Morán, Synthesis and adsorption properties of activated carbons from biomass of *Prunus domestica* and *Jacaranda mimosifolia* for the removal of heavy metals and dyes from water, Ind. Crops Prod. 42 (2013) 315–323.
[7] X.J. Zhou, A. Buekens, X.D. Li, M.J. Ni, K.F. Cen, Adsorption of polychlorinated dibenzo-p-dioxins/dibenzofurans on activated carbon from hexane, Chemosphere 144 (2016) 1264–1269.
[8] N. Ferrera-Lorenzo, E. Fuente, I. Suárez-Ruiz, B. Ruiz, Sustainable activated carbons of macroalgae waste from the Agar-Agar industry. Prospects as adsorbent for gas storage at high pressures, Chem. Eng. J. 250 (2014) 128–136.
[9] Z. Chen, K. Li, L. Pu, The performance of phosphorus (P)-doped activated carbon as a catalyst in air-cathode microbial fuel cells, Bioresour. Technol. 170 (2014) 379–384.
[10] A.S. Mestre, R.A. Pires, I. Aroso, E.M. Fernandes, M.L. Pinto, R.L. Reis, M.A. Andrade, J. Pires, S.P. Silva, A.P. Carvalho, Activated carbons prepared from industrial pre-treated cork: sustainable adsorbents for pharmaceutical compounds removal, Chem. Eng. J. 253 (2014) 408–417.
[11] D. Kołodyńska, R. Wnętrzak, J.J. Leahy, M.H.B. Hayes, W. Kwapiński, Z. Hubicki, Kinetic adsorptive characterization of biochar in metal ions removal, Chem. Eng. J. 197 (2012) 295–305.
[12] J. Lehmann, Bio-energy in the black, Front. Ecol. Environ. 5 (2007) 381–387.
[13] S. Meyer, B. Glaser, P. Quicker, Technical, economical, and climate-related aspects of biochar production technologies: a literature review, Environ. Sci. Technol. 45 (2011) 9473–9483.
[14] M. Ahmad, S.S. Lee, X. Dou, D. Mohan, J.K. Sung, J.E. Yang, Y.S. Ok, Effects of pyrolysis temperature on soybean stover- and peanut shell-derived biochar properties and TCE adsorption in water, Bioresour. Technol. 118 (2012) 536–544.
[15] A. Shah, M.J. Darr, D. Dalluge, D. Medic, K. Webster, R.C. Brown, Physicochemical properties of bio-oil and biochar produced by fast pyrolysis of stored single-pass corn stover and cobs, Bioresour. Technol. 125 (2012) 348–352.
[16] M.C. Rillig, M. Wagner, M. Salem, P.M. Antunes, C. George, H.G. Ramke, M.M. Titirici, M. Antonietti, Material derived from hydrothermal carbonization:

Effects on plant growth and arbuscular mycorrhiza, Appl. Soil Ecol. 45 (2010) 238–242.
[17] X. Tan, Y. Liu, G. Zeng, X. Wang, X. Hu, Y. Gu, Z. Yang, Application of biochar for the removal of pollutants from aqueous solutions, Chemosphere 125 (2015) 70–85.
[18] H.S. Kambo, A. Dutta, A comparative review of biochar and hydrochar in terms of production, physico-chemical properties and applications, Renew. Sustain. Energy Rev. 45 (2015) 359–378.
[19] S. Malghani, G. Gleixner, S.E. Trumbore, Chars produced by slow pyrolysis and hydrothermal carbonization vary in carbon sequestration potential and greenhouse gases emissions, Soil Biol. Biochem. 62 (2013) 137–146.
[20] B. Chen, Z. Chen, Sorption of naphthalene and 1-naphthol by biochars of orange peels with different pyrolytic temperatures, Chemosphere 76 (2009) 127–133.
[21] M.P. McHenry, Agricultural bio-char production, renewable energy generation and farm carbon sequestration in Western Australia: certainty, uncertainty and risk, Agric. Ecosyst. Environ. 129 (2009) 1–7.
[22] M. Zhang, B. Gao, Removal of arsenic, methylene blue, and phosphate by biochar/AlOOH nanocomposite, Chem. Eng. J. 226 (2013) 286–292.
[23] S. Kumar, V.A. Loganathan, R.B. Gupta, M.O. Barnett, An assessment of U(VI) removal from groundwater using biochar produced from hydrothermal carbonization, J. Environ. Manage. 92 (2011) 2504–2512.
[24] W. Hartley, N.M. Dickinson, P. Riby, N.W. Lepp, Arsenic mobility in brownfield soils amended with green waste kompost or biochar and planted with Miscanthus, Environ. Pollut. 157 (2009) 2654–2662.
[25] D. Matovic, Biochar as a viable carbon sequestration option: global and Canadian perspective, Energy 36 (2011) 2011–2016.
[26] D. Mohan, A. Sarswat, Y.S. Ok, C.U. Pittman Jr., Organic and inorganic contaminants removal from water with biochar, a renewable, low cost and sustainable adsorbent – a critical review, Bioresour. Technol. 160 (2014) 191–202.
[27] M. Zhang, B. Gao, Y. Yao, Y. Xue, M. Inyang, Synthesis of porous MgO-biochar nanocomposites for removal of phosphate and nitrate from aqueous solutions, Chem. Eng. J. 210 (2012) 26–32.
[28] P. Regmi, J.L. Garcia Moscoso, S. Kumar, X. Cao, J. Mao, G. Schafran, Removal of copper and cadmium from aqueous solution using switchgrass biochar produced via hydrothermal carbonization process, J. Environ. Manage. 109 (2012) 61–69.
[29] X. Chen, G. Chen, L. Chen, Y. Chen, J. Lehmann, M.B. McBride, A.G. Hay, Adsorption of copper and zinc by biochars produced from pyrolysis of hardwood and corn straw in aqueous solution, Bioresour. Technol. 102 (2011) 8877–8884.
[30] W. Zhang, S. Mao, H. Chen, L. Huang, R. Qiu, Pb(II) and Cr(VI) sorption by biochars pyrolyzed from the municipal wastewater sludge under different heating conditions, Bioresour. Technol. 147 (2013) 545–552.
[31] <http://www.coaltecenergy.com/biochar/>.
[32] <http://www.radus.pl/pdf/wegiel/AC20-AC20G.pdf>.
[33] M.V. Lopez-Ramon, F. Stoeckli, C. Moreno-Castilla, F. Carraso-Marin, On the characterization of acidic and basic surface sites on carbons by various techniques, Carbon 37 (1999) 1215–1221.
[34] S. Lagergren, Zur theorie der sogenannten adsorption gelosterstoffe, Kungliga Svenska Vetenskapsakademiens Handlingar 24 (1898) 1–39.
[35] Y.S. Ho, G. McKay, Sorption of dye from aqueous solution by peat, Chem. Eng. J. 70 (1998) 115–124.
[36] W.J. Weber, J.C. Morris, Kinetics of adsorption on carbon from solution, J. Sanitary Eng. Div. 89 (1963) 31–60.
[37] C. Tan, Z. Yaxin, W. Hongtao, L. Wenjing, Z. Zeyu, Z. Yuancheng, R. Lulu, Influence of pyrolysis temperature on characteristics and heavy metal adsorptive performance of biochar derived from municipal sewage sludge, Bioresour. Technol. 164 (2014) 47–54.
[38] A.W. Samsuri, F. Sadegh-Zadeh, B.J. Seh-Bardan, Adsorption of As(III) and As(V) by Fe coated biochars and biochars produced from empty fruit bunch and rice husk, J. Environ. Chem. Eng. 1 (2013) 981–988.
[39] T.M. Abdel-Fattah, M.E. Mahmoud, S.B. Ahmed, M.D. Huff, J.W. Lee, S. Kumar, Biochar from woody biomass for removing metal contaminants and carbon sequestration, J. Ind. Eng. Chem. 22 (2015) 103–109.
[40] W.K. Kim, T. Shim, Y.S. Kim, S. Hyun, C. Ryu, Y.K. Park, J. Jung, Characterization of cadmium removal from aqueous solution by biochar produced from a giant *Miscanthus* at different pyrolytic temperatures, Bioresour. Technol. 138 (2013) 266–270.
[41] X.J. Tong, J.Y. Li, J.H. Yuan, R.K. Xu, Adsorption of Cu(II) by biochars generated from three crop straws, Chem. Eng. J. 172 (2011) 828–834.
[42] X. Dong, L.Q. Ma, Y. Li, Characteristics and mechanisms of hexavalent chromium removal by biochar from sugar beet tailing, J. Hazard. Mater. 190 (2011) 909–915.
[43] J. Wang, B. Chen, Adsorption and coadsorption of organic pollutants and a heavy metal by graphene oxide and reduced graphene materials, Chem. Eng. J. 281 (2015) 379–388.
[44] D. Özçimen, A. Ersoy-Meriçboyu, Characterization of biochar and bio-oil samples obtained from carbonization of various biomass materials, Renewable Energy 35 (2010) 1319–1324.
[45] X. Xu, X. Cao, L. Zhao, Comparison of rice husk- and dairy manure-derived biochars for simultaneously removing heavy metals from aqueous solutions: role of mineral components in biochars, Chemosphere 92 (2013) 955–961.
[46] Y. Yang, Z. Wei, X. Zhang, X. Chen, D. Yue, Q. Yin, L. Xiao, L. Yang, Biochar from *Alternanthera philoxeroides* could remove Pb(II) efficiently, Bioresour. Technol. 171 (2014) 227–232.
[47] S.I. Mussatto, M. Fernandes, G.J.M. Rocha, J.J.M. Órfão, J.A. Teixeira, I.C. Roberto, Production, characterization and application of activated carbon from brewer's spent grain lignin, Bioresour. Technol. 101 (2010) 2450–2457.
[48] V. Fierro, V. Torné-Fernández, A. Celzard, Kraft lignin as a precursor for microporous activated carbons prepared by impregnation with ortho-phosphoric acid: synthesis and textural characterisation, Microporous Mesoporous Mater. 92 (2006) 243–250.
[49] A. Behnamfard, M. Mehdi Salarirad, F. Vegliò, Removal of Zn(II) ions from aqueous solutions by ethyl xanthate impregnated activated carbons, Hydrometallurgy 144–145 (2014) 39–53.
[50] D. Mohan, H. Kumar, A. Sarswat, M. Alexandre-Franco, C.U. Pittman Jr., Cadmium and lead remediation using magnetic oak wood and oak bark fast pyrolysis bio-chars, Chem. Eng. J. 236 (2014) 513–528.
[51] Y. Sun, B. Gao, Y. Yao, J. Fang, M. Zhang, Y. Zhou, H. Chen, L. Yang, Effects of feedstock type, production method, and pyrolysis temperature on biochar and hydrochar properties, Chem. Eng. J. 240 (2014) 574–578.
[52] M. Li, Q. Liu, L. Guo, Y. Zhang, Z. Lou, Y. Wang, G. Qian, Cu(II) removal from aqueous solution by Spartina alterniflora derived biochar, Bioresour. Technol. 141 (2013) 83–88.
[53] S. Vilvanathan, S. Shanthakumar, Biosorption of Co(II) ions from aqueous solution using *Chrysanthemum indicum*: kinetics, equilibrium and thermodynamics, Process Saf. Environ. Prot. 96 (2015) 98–110.
[54] W. Ding, X. Dong, I.M. Ime, B. Gao, L.Q. Ma, Pyrolytic temperatures impact lead sorption mechanisms by bagasse biochars, Chemosphere 105 (2014) 68–74.
[55] H. Yanagisawa, Y. Matsumoto, M. Machida, Adsorption of Zn(II) and Cd(II) ions onto magnesium and activated carbon composite in aqueous solution, Appl. Surf. Sci. 256 (2010) 1619–1623.
[56] Y. Xue, B. Gao, Y. Yao, M. Inyang, M. Zhang, A.R. Zimmerman, K.S. Ro, Hydrogen peroxide modification enhances the ability of biochar (hydrochar) produced from hydrothermal carbonization of peanut hull to remove aqueous heavy metals: batch and column tests, Chem. Eng. J. 200–202 (2012) 673–680.
[57] Z. Liu, F. Zhang, Removal of lead from water using biochars prepared from hydrothermal liquefaction of biomass, J. Hazard. Mater. 167 (2009) 933–939.
[58] A. Abdolali, H.H. Ngo, W. Guo, J.L. Zhou, B. Du, Q. Wei, X.C. Wang, P.D. Nguyen, Characterization of a multi-metal binding biosorbent: chemical modification and desorption studies, Bioresour. Technol. 193 (2015) 477–487.
[59] D. Ozdes, A. Gundogdu, B. Kemer, C. Duran, H.B. Senturk, M. Soylak, Removal of Pb(II) ions from aqueous solution by a waste mud from copper mine industry: equilibrium, kinetic and thermodynamic study, J. Hazard. Mater. 166 (2009) 1480–1487.
[60] A. Bogusz, P. Oleszczuk, R. Dobrowolski, Application of laboratory prepared and commercially available biochars to adsorption of cadmium, copper and zinc ions from water, Bioresour. Technol. 196 (2015) 540–549.